

The effect of 3D weaving and consolidation on carbon fiber tows, fabrics, and composites

E Archer, S Buchanan, AT McIlhagger and JP Quinn

Abstract

This article investigates the damage imparted on load-bearing carbon fibers during the 3D weaving process and the subsequent compaction behavior of 3D woven textile preforms. The 3D multi-layer reinforcements were manufactured on a textile loom with few mechanical modifications to produce preforms with fibers orientated in the warp, weft, and through-the-thickness directions. Tensile tests were conducted on three types of commercially available carbon fibers, 12k HTA, 6k HTS, and 3k HTS in an attempt to quantify the effect of fiber damage induced during the 3D weaving process on the mechanical and physical performance of the fiber tows in the woven composite. The tests were conducted on fiber tows sampled from different locations in the manufacturing process from the bobbin, through the creel and loom mechanism, to the final woven fabric. Mechanical and physical testing were then conducted to quantify the tow geometry, orientation and the effect of compaction during manufacture of two styles of 3D woven composite by vacuum-assisted resin transfer molding (VaRTM).

Keywords

3D weaving, carbon fiber, fabric

Introduction

New commercial aircraft programmes such as the Airbus A350, Boeing 787, Dreamliner or Bombardier C-Series have increased the demand for polymer composite primary aircraft structures with a gradual move towards the use of liquid molding resin transfer technology. This generally requires the use of a woven or stitched form of dry fabric rather than the more traditional methods of pre-impregnation of unidirectional tape. Woven textile reinforced composites allow the introduction of specific material properties into the final component that can provide a reduction in manufacturing cost. However, woven composites materials are susceptible to transverse impact loading which causes laminas to become delaminated.¹ Various methods have been developed to improve the impact tolerance including z-pinning, selective interlayers and hybrids, protective layers or resin toughening. One method that is becoming increasingly successful is to reinforce composites with a fiber that connects the layers together running from the upper to lower surface

of the laminate. Mouritz et al.² stated that 3D woven composites have higher ballistic damage resistance and impact tolerance resistance than 2D materials, higher tensile strain and strain-to-failure values, and also higher interlaminar fracture toughness; this might be beneficial in the design of primary aircraft structures where the limiting design criteria is compression after impact. It might also resist delaminations caused by bolt bearing loads at bolted joints or through-thickness tension failure at stringer runouts. Ding et al.³ showed that 3D composites performed significantly better in fatigue than 2D composites. Quinn et al.⁴ also point out a fundamental difference and advantage that 3D

Engineering Composites Research Centre, University of Ulster, Northern Ireland.

Corresponding author:

E Archer, Engineering Composites Research Centre, University of Ulster, Jordanstown BT37 0QB, Northern Ireland
Email: e.archer@ulster.ac.uk

reinforcements has over 2D plied lay-up. With a 2D lay-up, the orientation of the plies is carried out during the loading of the cure tool. Therefore care and considerable time must be taken to ensure the correct orientation of the final part. With 3D woven reinforcement the orientation of the tows is controlled by the design of the fabric which Mouritz et al.² state makes it possible to create complex near-net-shape preforms that can be less expensive and simpler to manufacture than 2D reinforced composites.

It has been suggested, however, that 3D woven composites generally exhibit lower in-plane properties due to degradation during manufacture, among other factors. The reduced mechanical performance is believed to result from crimping and misalignment of the load-bearing fibers by insertion of the z-binder yarns during weaving and distortion of the 3D architecture by compaction during the resin impregnation and cure cycle. In addition, it has been discovered that damage to fibers during weaving also degrades the in-plane properties of the 3D composite.⁵ During the weaving process, the fibers are bent, twisted, distorted and repeatedly abraded as they move through the creel and loom. This damage can come in two forms: fiber breakage or abrasion caused by fibers rubbing against other fibers and the loom machinery itself. It is believed to be due to the stiff and brittle nature of carbon fiber tows that there is a propensity for damage to occur during the weaving process; both the modulus and the strength of the composite are controlled substantially by the fiber, so this weaving damage will affect the mechanical properties of the composite structure.

Several researchers have published work characterizing damage caused to glass yarns by 3D weaving.^{5,6} The authors determined the influence of the weaving damage on the tensile stiffness, strength, and failure mechanisms of fiber yarns. The results showed that the most extensive damage occurred during the tensioning and beat-up stage, and suggested that the weaving caused a reduction in strength of dry load-bearing yarns in 3D glass preforms of approximately 30%. The same behavior is found in the z-binder yarn having a reduction of up to 50% in tensile strength. They concluded that this greater loss in strength of the z-binder may be due to the fact that this yarn is bent more severely than the warp yarn during weaving, and also that generally the z-binder is of smaller thickness than that of the warp yarn. However, tension tests were performed on both 2D and 3D woven composites for comparison. It was discovered that the Young's Modulus of the 3D woven composite was significantly lower; it was suggested that this was due to the distortion and crimp of the load-bearing yarns by the z-binders.⁶ The conclusion of this work suggests that loom modifications are needed to reduce abrasion since it has

been shown that fiber rubbing against the actual machinery is the biggest cause of damage to the fiber. It has been proposed that one possible modification is to cover the machinery surface in contact with the yarn with a wear-resistant material having a low co-efficient of friction, in order to reduce abrasion.

Studies have investigated the effect of fiber damage on carbon fiber tows caused by 3D weaving.⁷ They tested two types of carbon fiber and determined that the tensile strength of the first grade was unaffected by weaving damage, and the second carbon yarns were reduced by up to 12% due to abrasion and bending. They also determined that the modulus was almost unaffected for both. However, when testing the composite, they found a large degradation in both strength and modulus caused by fiber misalignment due to crimping.

The loss in yarn strength due to weaving damage is a cause for concern, especially when these materials are to be used for structural components. Any increase in variation of b-basis scatter caused by weaving inconsistencies would require further knockdown factors and redundancy to be applied in design calculations. This could potentially erode the benefits offered by this technology. More research is needed, therefore, to quantify the importance of this damage, to reduce damage levels by further analysis, and to develop the 3D weaving process. It would also be beneficial if a better understanding was sought as to the mechanisms of fiber misalignment due to crimping.

The compaction of dry fibers is unique to RTM and other resin infusion processes. This gives rise to the complex behavior of the fiber on the bundle level.⁸ The compaction of the fibers in all cases results in changes in fiber volume fraction, porosity, and pore dimensions. This in turn has effects on the processibility of the reinforcement by affecting the permeability and, consequently, resin flow. Additionally the fiber volume fraction will influence the mechanical properties of the finished composite.⁹ In recent research specifically investigating 3D woven composites, the author indicated that an optimum compaction level exists, after which deformation of the tows and deviation from the designed architecture can cause a detraction in mechanical properties.¹⁰

The consolidation of the reinforcement compresses the fabric reinforcement, resulting in a reduction in fabric thickness but an increase of the composite's final fiber volume fraction (V_f) that influences the calculated mechanical performance from experimental analysis and modeling of the mechanical properties. The dry fabric compression test has been widely used to establish semi-empirical relationships of 2D woven fabric assemblies. Predictive equations for example, developed by Quinn and Randall¹¹ describe a linear

relationship between the V_f and the square root of the pressure (P) on the sample:

$$V_f = k_1 + k_2 \sqrt{P}. \quad (1)$$

Other authors developed a power law relationship between the applied pressure and V_f^9 , which has subsequently shown to be applicable to the compression of 3D woven orthogonal bound fabric reinforcements¹²:

$$P = cV_f^m, \quad (2)$$

where P , c , V_f , and m are, respectively, pressure, empirical constant, fiber volume fraction (%), and power law index number. The empirical constants c and m are determined by taking natural log of the pressure and V_f data. This produces a linear graph where the relationship between the $\ln P$ and $\ln V_f$ are analogous to the equation of the straight line graph, that is $y = mx + c \equiv \ln P = \ln c + \ln V_f^m$. The constants ' c_p ' and ' n_p ' in the equation are calculated from the graph of pressure vs. V_f . The model does not relate these constants to any physical section of the fabric structure and hence it is a limitation of this empirical approach. Compression tests must be performed prior to any calculation on the required pressure to achieve a specified V_f .

In a review of the work by previous authors, a number of factors have been identified as affecting the compressive qualities of a woven textile. A summary of these is shown in Table 1.

Table 1. Issues associated with compression

Binder density – the number of through the thickness tows per unit area
Initial fabric thickness
Reorganization of the fabric structure

Table 2. Details of fabrics

	Warp	Weft	Binder content (%)	Binder type	Areal weight (g/m ²)
Angle interlock	2 × 12k HTS	12k HTS	6	6k HTA	2720
Layer-to-layer interlock	2 × 12k HTS	12k HTS	6	3k HTA	2720

Table 3. Material supplier data for filament yarn

	Tensile strength (MPa)	Tensile modulus (GPa)
HTA	3950	238
HTS	4300	240

This work will investigate the compaction modes and use this empirical approach to determine whether the relationships defined in the literature can be applied to complex 3D woven fabrics with small binder content and low levels of off-the-loom crimp, and whether the difference between two fabrics with similar warp and weft fibers but different binding patterns is discernable.

Experimental

The 3D multi-layer woven reinforcements were designed using the X-Sectional design system to provide a representation of the structure, detailing the relative positions of the yarns and also generating the lifting plan to operate a Jacquard controlled loom. Fabrics were then manufactured on a conventional textile loom with mechanical modifications to allow the addition of z-binder yarns and limit fiber damage. Reinforcements with fibers orientated in the warp, weft, and through-the-thickness directions were produced (Table 2). The loom used was a Dataweave loom with Jacquard controller incorporating 1152 hooks. Two specific weave architectures that consist of long continuous lengths of tows for maximum strength in the 0°/90° directions and have angle interlock binding configurations in order to suppress delaminations were manufactured. Comparatively, these structures possess very low levels of crimp in the warp stuffer and weft filler tows. Both fabrics have four layers of warp and five of weft, while maintaining a 1:1 warp to weft ratio, with the binder running in the warp direction.

For the manufacture of the two fabric types the fiber bundles were initially rewound from large bobbins supplied by the fiber manufacturer onto smaller packages for addition to the creel (Table 3). A high speed single head winder was used. It was observed that some fiber damage was caused during this step. Each package was placed on the creel and the fiber was passed

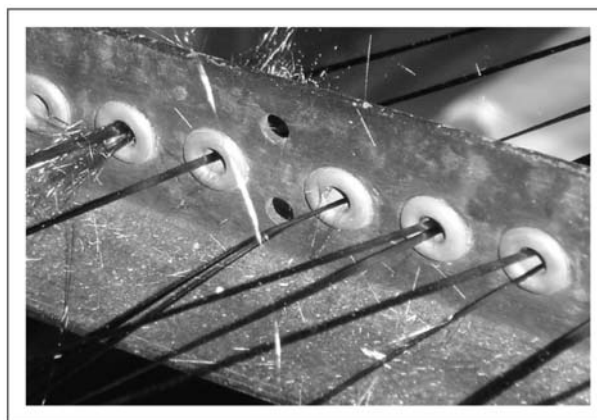


Figure 1. Weaving damage at creel eye board.

through ceramic guides on the creel (Figure 1). The warp stuffer ends were doubled up at the ‘creel eye,’ which are ceramic guides at the end of the creel that were installed to limit entanglement of fiber bundles. Passive tensioning devices were added to each bobbin to apply tension to each warp stuffer yarn. This reduced the chances of individual tows becoming entangled before the eye board, and to aid in the movement of binders past one another in the harness (hooks).

Dry yarn specimens were removed from the process for assessment of tensile properties. Tensile properties for 12k, 6k, and 3k were determined in several regions. This included:

- As received virgin yarn
- Rewound on creel
- After hooks
- Out of fabric.

Care was taken when removing warp and binder yarns from the woven fabrics. The fabrics were dissected using scissors, scalpel blades, and tweezers.

The degree of crimp within the uncompressed fabric structure was measured for the warp, weft, and binder tows. Crimp measurements were made in accordance with BS 2863:1984.¹³ The yarns straightened as described in the standard to determine the straight length. Crimp (C) is calculated using the equation below:

$$C = \frac{L - L_o}{L_o}, \quad (3)$$

where L is the mean measured length of 10 threads removed from the fabric and L_o is the length occupied by the tow in the fabric, that is the flap width.

Instron Cord Capstan grips were used for clamping dry fibers during tensile testing; each grip has a round capstan with a right-hand spiral grooved surface. The capstan is split axially into two halves, one half being stationary and the other movable. The specimen is wound from the outside of the capstan towards the center before being passed through the split halves where it is clamped. The groove completes 2.5 turns around the capstan, which allows two full turns for distributing the specimen load and stress concentration. The grips self-tighten as load is applied to the specimen.

The grips were loaded onto a Zwick Z100 universal tester. A gage length of 75 mm of fiber between each clamp was used, with a test speed of 4 mm/min.¹⁴

To determine the dry compressive properties of the fabric, each of the fabric samples was cut to a size of $100 \times 100 \text{ mm}^2$. Samples were cut carefully on a glass cutting surface using a scalpel and a steel template. The cutting template had slots added at each corner to allow the blade to run further than 100 mm. This ensured a

clean cut was made. After cutting, the sample was loaded into the compression platens. The compression platens were secured into a Zwick Z100 universal tester. A speed of 1 mm/min was selected as the rate of application of load up to a point representing 200 kPa pressure. With the platens secured into the tester, the top platen was brought down until a preload of 20 N registered on the fabric sample. The 20 N over the area of the sample is equal to a pressure of 2 kPa. During the compression of the sample, the movement of the crosshead and the force applied to the sample were recorded. Equation (4) calculates the change in thickness for each sample under compression:

$$T_c = T_o - C_{abs}, \quad (4)$$

where T_c , T_o , and C_{abs} are, respectively, compressed thickness, initial fabric thickness, and crosshead movement absolute.

Optical microscopy was carried out on the unconsolidated fabric and consolidated fabric samples in order to ascertain the geometric characteristics of the fabric in the ‘off-loom state’ compared to the consolidated composite that was compressed at 100 kPa during vacuum-assisted resin transfer molding (VaRTM) processing. Samples measuring $150 \times 150 \text{ mm}^2$ were taken from the fabric preform that was removed from the loom. The fabric samples were set in degassed resin at atmospheric pressure in order to stabilize and maintain the geometric arrangement of yarns in the unconsolidated fabric. Consolidated samples were also cut for the composite plaque that was produced using VaRTM. The samples were subsequently sectioned from the unconsolidated and consolidate plaques along the warp and weft directions and polished progressively using silicon carbide paper, which enabled optical microscopy. Micrographs were taken of the compressed and uncompressed composite samples in the warp and weft direction.

Finally, several woven composite plaques were manufactured using the VaRTM method. A caul plate was used in conjunction with a flexible membrane to consolidate the fabric reinforcements under full vacuum, prior to the injection of resin by peripheral gating at a tool temperature of 75°C. Araldite LY564 and Hardener HY2954 (based on bisphenol A epoxy and a cycloaliphatic amine hardener) was mixed and degassed at 2.86:1 by weight before the transfer of the resin. After injection, a ramp was applied up to 100°C. The temperature was held isothermal for 60 min; the composite plaque was then de-molded and post-cured for a further 180 min at 140°C. Fiber volume fraction was measured using the density buoyancy method in which the sample’s mass in air is recorded before weighing the sample again in distilled

water according to ASTM D792-91.¹⁵ Therefore, having obtained the specific gravity and knowing the densities of the constituent parts, that is, the fiber and resin, the percentage content of the fibers was calculated. It was found to be approximately 55% (St. dev. 1.60) for both composite weave architectures. Tensile specimens from both woven composite plaques were removed and tensile tested in the warp and weft direction on a Zwick Z100 universal tester. The testing was performed to CRAG standard 300.¹⁶ An MTS 632.85F biaxial extensometer was used to determine tensile modulus.

Results and discussion

Table 4 shows the tensile strength of dry yarns sampled from four stages in the weaving process. There is less than 3% difference in the tensile strength caused by weaving damage between the three fiber types. In these fabrics, the 12k stuffer follows a path with very little crimp whereas both the 6k and 3k binders follow a more crimped binding path; albeit a much less crimped path than that of the orthogonal bound fabrics reported by other authors in the area.¹⁰ The binder in the orthogonal fabrics goes directly from top layer to bottom layer, whereas the binders in the fabrics analyzed here go from top layer to bottom layer at an angle. The degree of crimp within the uncompressed fabric structure was found to be less than 0.5% for the warp stuffers and weft fillers, whereas the binders in the uncompressed angle interlock and layer-to-layer fabrics possessed 4.2% and 3.4% of crimp, respectively.

All three yarn types were found to experience a 9–10% drop in tensile strength from virgin (as received) properties to properties found in dry yarns dissected from the fabric.

Table 4 shows that the dry yarn damage is induced at each stage, with an initial degradation in tensile properties of approximately 5% in tensile strength from virgin fiber to rewound fiber, 1.5% degradation from the rewound fiber to the fiber at the hooks, and finally 2.8% degradation in properties from the loom fibers to the fabric fibers. These results indicate that on average there was an overall degradation of 9.4% from

the as-received virgin fiber to fiber extracted from the woven fabric.

The displacement of the crosshead was recorded to determine tensile modulus of the dry yarns. It was found that there was little variation in modulus due to weaving damage. This agrees with the findings of Lee et al.⁶

In each case the largest reduction in dry yarn tensile strength is observed at the rewinding stage (5–6%). This is a high speed process using a single-head winder. The actual weaving process only imparts approximately a further 4% knockdown in dry fiber tensile properties. Prior to this work, several modifications were made to the loom to ensure limited weaving damage. For these fabrics the loom was running at a much slower rate than a conventional textile loom. The loom was run at approximately 120 picks per minute whereas a conventional textile loom would run at up to 600 picks per minute. It is expected that as the weaving production speed is increased in terms of picks per minute, greater damage will be caused as the carbon fiber yarns move through the loom mechanism at a greater rate.

As expected, all three yarn types possessed much lower virgin (as-received) properties than those values given by the material supplier.

Figures 2 and 3 illustrate the organization of the warp and weft tows as well as the binder tows within each structure in the off-the-loom state under zero load. For both fabrics it is clear that the warp and weft stuffers generally display a straight path with symmetrical regularity. However, even in the uncompressed state it appears that the vertical alignment of the warp stuffer in the layer-to-layer fabric (Figure 2(b)) is not as ordered as the angle interlock fabric (Figure 3(b)). It is thought that the addition of a 3k layer-to-layer binder on each warp layer causes a more compact off-the-loom fabric than the angle interlock design. This encourages the larger warp stuffers to reorganize into a thinner vertical height (fabric thickness), squashing the tow into a more lenticular shape and nesting with lateral movement relative to the stuffer on the layer above.

When comparing the loom state fabric (Figure 2) to the VaRTM manufactured composite (Figure 4) for the

Table 4. Tensile strength of dry yarns sampled from four stages in the weaving process

Fiber state	12k stuffer tensile strength (MPa)	6k binder tensile strength (MPa)	3k binder tensile strength (MPa)
Virgin	2210	2010	1998
Rewound on creel	2100	1915	1880
After hooks	2070	1871	1860
Woven	1985	1827	1820
Standard deviation	80	61	63
CV (%)	7	8	10

layer-to-layer fabric, it is clear that the weft fillers in the loom state fabric are much more ordered in the vertical direction than in the composite. During VaRTM manufacture, the application of pressure causes nesting in both warp and weft directions. When comparing the loom state fabric (Figure 3) to the VaRTM manufactured composite (Figure 5) for the angle interlock fabric, there appears to be a change in tow cross-sectional shape in both the warp and weft directions. In general the warp and weft tows remain straight although the weft filler exhibited more crimp in the composite than the warp stuffer.

The compressed samples illustrate how the compression of the preform causes reorganization of the tows within the structure. The weft tows have the freedom to move within the binder points in the structure and this movement can be affected by characteristics of the fabric structure, namely the frequency of the binder yarns within the structure.

The micrographs in Figure 4 for the layer-to-layer in both longitudinal and transverse directions show a large degree of nesting in the warp stuffers. It is thought that this could be due to the difference in size between the large stuffer tow and the smaller 3k binder tow.

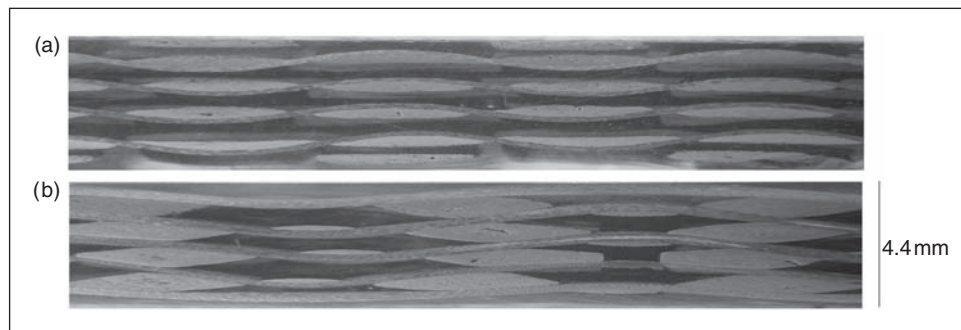


Figure 2. Longitudinal (a) and transverse (b) micrograph of layer-to-layer loom state composite.

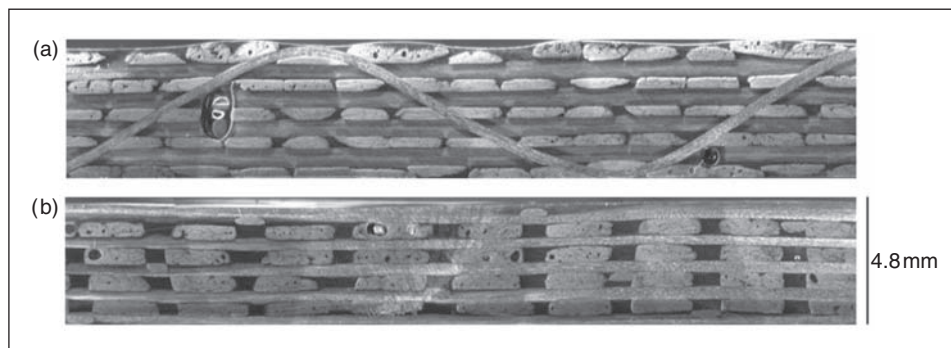


Figure 3. Longitudinal (a) and transverse (b) micrograph of angle interlock loom state composite.

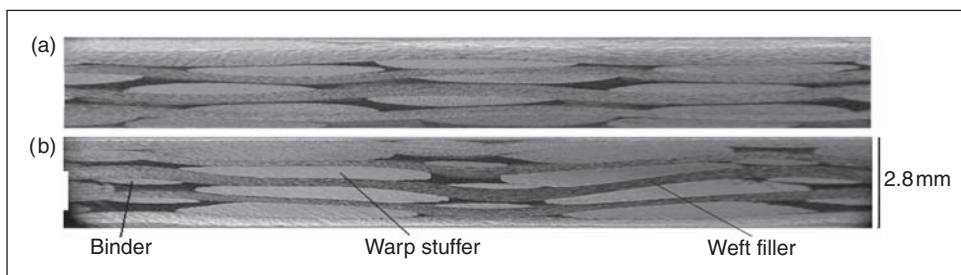


Figure 4. Longitudinal (a) and transverse (b) micrograph of layer-to-layer composite.

There are also resin rich areas around the binder. However, as a binder is present at each layer, the resin rich area is smaller than in the angle interlock fabrics. The layer-to-layer composite exhibits a higher degree of crimp in the weft filler compared to the angle interlock composite. Also, due to the restriction on lateral movement caused by the binder on each warp layer, the warp stuffer tows tended to deform their lenticular shape, elongating and conforming to the crimp of the weft filler tows.

Figure 5 shows a micrograph of the angle interlock composite. It is clear that the warp stuffers are very straight with little crimp. However, the weft fillers exhibit crimp to a greater extent. It is thought that this is due to a lack of tension exerted during the weaving process with the insertion of the weft yarn by the loom rapier. This lack of tension in the weft direction accommodates the nesting effects caused by the binders which cross over the weft yarns at the surface layer of the fabric, bending the weft yarn down under compression from the caul plate during composite manufacture. Resin-rich areas were also observed between warp stuffers in the space that is occupied by the binder on other weft layers. These resin rich areas will be difficult to eliminate with this design of fabric due to the binder pitch.

Physically, the fabric structures handle very differently. Layer-to-layer is the most tightly woven and when handling it the structure remains intact, whereas care must be taken when handling angle interlock as the loose weave structure means tows of fiber moving quite a lot. This can result in the detaching of tows from the edges of the structure.

A plot of the variation in V_f against the applied pressure measured using the empirical approach explained above is shown in Figure 6. As expected, fiber volume increases with applied pressure. The pressure range used in this work was quite low, stopping at a maximum pressure of 200 kPa. On application of higher pressure the V_f value for the reinforcement would increase until a point of maximum packing. At the point of maximum packing all nesting of tows and filaments has taken place

and no more compression of the fabric structure could occur. Unless the pressure on the preform is closely controlled at this point, the fibers would begin to damage. This damage may reduce the mechanical properties of the composite component. This is one of the benefits of using lower pressure for composite manufacture with 3D woven fabrics.

The behavior of both fabrics can be fitted to a power law relationship as described above. The subsequent model provides the facility for a determination of required pressure on the preform during processing to achieve a specific V_f . The results from compression tests have shown that the V_f increases with application of pressure to the sample for these 3D woven fabrics with small binder content and low levels of off-the-loom crimp in a similar way as with other fabrics tested by various researchers. However, the results indicate that the orientation or type of binder has little effect on the compressive properties of a 3D woven composite when it is in a small percentage and the compression of the structure is dictated by the rearrangement of the warp and weft stuffers within the structure. Both the angle interlock and the layer-to-layer preforms exhibit similar dry compressive properties but by examination of the micrographs, it is clear that the rearrangement of the warp and weft stuffers within the structure differs depending on binder architecture.

Table 5 shows the strength and stiffness values for the two composite materials in the warp (x) and weft (y) directions. It was found that the angle interlock composite possessed superior strength and stiffness values in both directions. In both of the 3D woven composite specimens, stiffness and strength were significantly lower in the weft direction than in the warp. The layer-to-layer composite was found to have a lower modulus and strength than the angle interlock composite. The layer-to-layer composite also exhibited a greater differential between warp and weft properties exhibiting a 26.9% reduction in modulus compared to the 12.3% exhibited by the angle interlock composite. Also, the angle interlock composite displayed a 19.2%

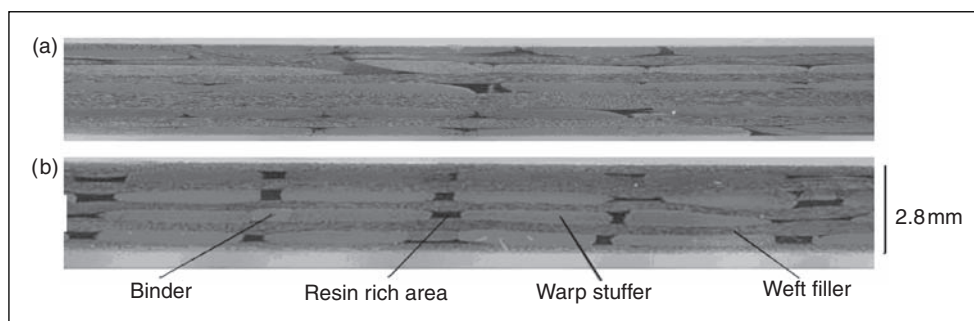


Figure 5. Longitudinal (a) and transverse (b) micrograph of angle interlock composite.

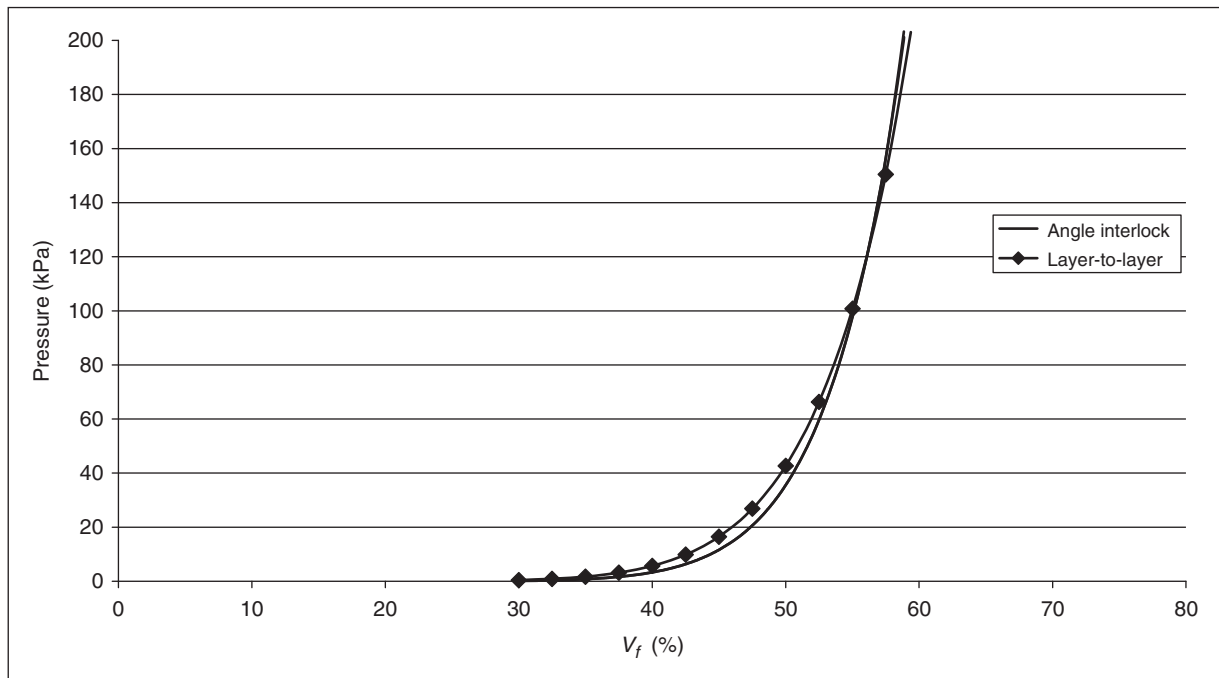


Figure 6. Dry fabric compression plot.

Table 5. Mechanical properties for woven composite specimens (55% fv)

Material	E_x (GPa)	E_y (GPa)	σ_x (MPa)	σ_y (MPa)
Angle interlock	65 ± 2.20	57 ± 1.50	861 ± 32	695 ± 21
Layer-to-layer	63 ± 2.7	46 ± 2.4	789 ± 47	485 ± 55

reduction in strength compared to a 37.8% reduction in the layer-to-layer strength value. Both these composites were manufactured using the same method, from pre-forms with the same yarns used in the warp and weft direction, producing the same areal weight. The only difference between the composites is the orientation and architecture and fiber type of the through-thickness binder. It is clear therefore that the careful selection of weave architecture is of paramount importance, as is the ability to understand the effect of changes in weave design. From the micrographs (Figures 4 and 5) it appears that the binder has an effect on the level of stuffer and filler crimp and in turn there is an inverse relationship between warp and weft crimp levels, strength, and modulus values.

Conclusions

It was found that the overall reduction in tensile strength for dry carbon fiber yarns attributed to weaving damage was 9–10%. This is much lower than the 30% reduction reported for glass fiber yarn and by

other researchers. It is also lower than the 12% reduction reported for carbon fiber yarns.

Surprisingly both the 12k stuffers and the 3k and 6k binders exhibited similar knock down in dry tensile strength due to weaving damage. All dry fibers were found to show virtually no reduction in stiffness throughout the weaving process.

The findings in this work indicate that the rewinding process plays a major part in the fiber damage, imparting an initial degradation of approximately 5% in tensile strength from virgin fiber to rewound fiber. Therefore, further work is required to investigate the mechanics of the rewinding process.

The compaction of these low crimp off-the-loom, small binder content 3D woven fabrics was found to adhere to the relationships defined in the literature. However, despite the marked difference in the reorganization of the fabric structure observed in the micrographs, it was difficult to differentiate between the two fabrics using this empirical approach.

The reorganization of the fabric structure, however, did appear to affect the tensile mechanical properties of the composite structure. For the 3D woven composite specimens a large variation between warp and weft direction values were found for both tensile strength and modulus. It appears that more tension is required to maintain straighter weft fillers during fabric manufacture and consolidation for composite manufacture. However, a compromise must be achieved between applying more tension to the inserted weft filler tows,

such that excessive crimp is not introduced into the warp stuffers. It was found that initial weave architecture design has a large influence on tensile mechanical strength properties. The angle interlock composite possessed superior strength and stiffness values in both directions despite the fact that the same percentage of binder and identical warp and weft fibers were used in both fabric types.

It is expected that as the weaving production speed is increased in terms of picks per minute, greater damage will be caused as the carbon fiber yarns travel through the loom mechanism at a greater rate. Also, changes in material, weaving process, and weave architecture will significantly affect damage caused; this must be quantified. Further work, therefore, is required to maintain the low levels of fiber damage while increasing fabric production rate.

Acknowledgments

This work was supported by the 3DSIMCOMS consortium in collaboration with the Technology Strategy Board. The Technology Strategy Board is a business-led executive non-departmental public body, established by the government. Its mission is to promote and support research into, and development and exploitation of, technology and innovation for the benefit of UK business, in order to increase economic growth and improve the quality of life. It is sponsored by the Department for Innovation, Universities and Skills (DIUS). Please visit www.innovateuk.org <http://www.innovateuk.org/> for further information.

References

1. Atas C and Liu D. Impact Response of woven composites with small weaving angles. *Int J Impact Eng* 2008; 35(2): 80.
2. Mouritz AP, Bannister MK, Falzon PJ and Leong KH. Review of applications for advanced three-dimensional fibre textile composites. *Composites Part A* 1998; 30(12): 1445.
3. Ding YQ, Yan Y, McIlhagger R and Brown D. Comparison of the fatigue behaviour of 2-D and 3-D woven fabric reinforced composites. *J Mater Process Technol* 1995; 55(3-4): 171.
4. Quinn JP, McIlhagger R, McIlhagger AT, Wilson S, Simpson D and Wenger W. The influence of binder tow density on the mechanical properties of spatially reinforced composites, Part 1 – Impact resistance. *Composites Part A* 2007; 38(3): 795.
5. Rudov-Clark S, Mouritz AP, Lee L and Bannister MK. Fibre damage in the manufacture of advanced three-dimensional woven composites. *Composites Part A* 2002; 34(10): 963.
6. Lee L, Rudov-Clark S, Mouritz AP, Bannister MK and Herzberg I. Effect of weaving damage on the tensile properties of three-dimensional woven composites. *Compos Struct* 2002; 57(1-4): 405.
7. Lee B, Leong KH and Herzberg I. Effect of weaving on the tensile properties of carbon fibre tows and woven composites. *J Reinf Plast Compos* 2001; 20(8): 652.
8. Simacek P and Karbahari VM. Notes on the modelling of perform compaction: I – micromechanics at the fibre bundle level. *J Reinf Plast Compos* 1996; 15: 86.
9. Saunders RA, Lekakou C and Bader MG. Compression and microstructure of fibre plain woven cloths in the processing of polymer composites. *Composites Part A* 1998; 29A: 443.
10. Stewart G, McIlhagger AT, Quinn JP and King S. An investigation into the effect of compaction on the mechanical performance of a 3D reinforced advanced composite. *Polym Polym Compos* 2007; 15(7): 535.
11. Quinn JA and Randall JE. Compliance of composite reinforcement materials. *I Meche* 1990; 3: 105.
12. Quinn J, McIlhagger R and McIlhagger AT. A modified system for design and analysis of 3D woven preforms. *Composites Part A* 2003; 34A: 6503.
13. BS 2863. *Method for determination of crimp of yarn in fabric*. London: British Standards Institution, 1984.
14. ASTM D4018-81. *Standard test method for tensile properties of continuous filament carbon and graphite yarns, strands, rovings, and tows*. Philadelphia: ASTM, 1981.
15. ASTM D792-91. *Standard test methods for density and specific gravity (relative density) of plastics by displacement*. Philadelphia: ASTM, 1991.
16. CRAG Standard Method 302. *Method of test for the tensile strength and modulus of multidirectional fibre reinforced plastics*. Philadelphia: ASTM, 1988.